Concise Synthesis of (–)-Veratramine and (–)-20-*epi*-Veratramine via Aromative Diels-Alder Reaction

Michael D. Zott, Daniel W. Zuschlag, and Dirk H. Trauner*

Department of Chemistry, University of Pennsylvania, Philadelphia, PA 19104, USA

ABSTRACT: A concise and convergent synthesis of the isosteroidal alkaloids veratramine and 20-*epi*-veratramine has been accomplished. A Horner-Wadsworth-Emmons olefination joins two chiral building blocks of approximately equal complexity and a transition-metal catalyzed intramolecular Diels-Alder cycloaddition-aromatization cascade constructs the tetrasubstituted arene. Other key steps include a highly diastereoselective crotylation of an *N*-sulfonyl iminium ion and an Eschenmoser fragmentation. The chiral building blocks developed for this synthesis could be used to access a range of additional isosteroidal alkaloids using our diversifiable strategy. Our work shows that 20-*epi*-veratramine is not identical with a natural product proposed to have that structure. The single crystal X-ray structures of veratramine and 20-*epi*-veratramine are reported.

Plants of the genus *Veratrum* and *Fritillaria* produce a variety of architecturally intriguing isosteroidal alkaloids, with over 150 natural products isolated and characterized to date (**Scheme 1A**).[1] Some of these exhibit potent biological activities, such as antitumor, antihypertension, and antiarrhythmia activity.[2,3,4] Structurally, they feature a tetracyclic 6/6/5/6 scaffold linked to a piperidine heterocycle. They are distinguished from each other through their oxidation patterns and the degree of unsaturation in their D-ring, which can be aromatic (*e.g.,* in veratramine, 20-*epi*-veratramine, and heilonine), partially saturated (*e.g.,* in cyclopamine, stenanzine, and hosukinidine) or fully saturated (*e.g.,* in ebeiedine and tortifoline). Further increasing their diversity, these alkaloids come in a bewildering array of configurational permutations with respect to stereocenters at C20, C22, C23, and C25. For instance, veratramine, stenanzine, and tortifoline feature the 20*(S)* configuration, whereas 20-*epi*-veratramine, ebeiedine, hosukinidine, and heilonine are 20*(R)* configured. The biological consequences of this variability are poorly understood.

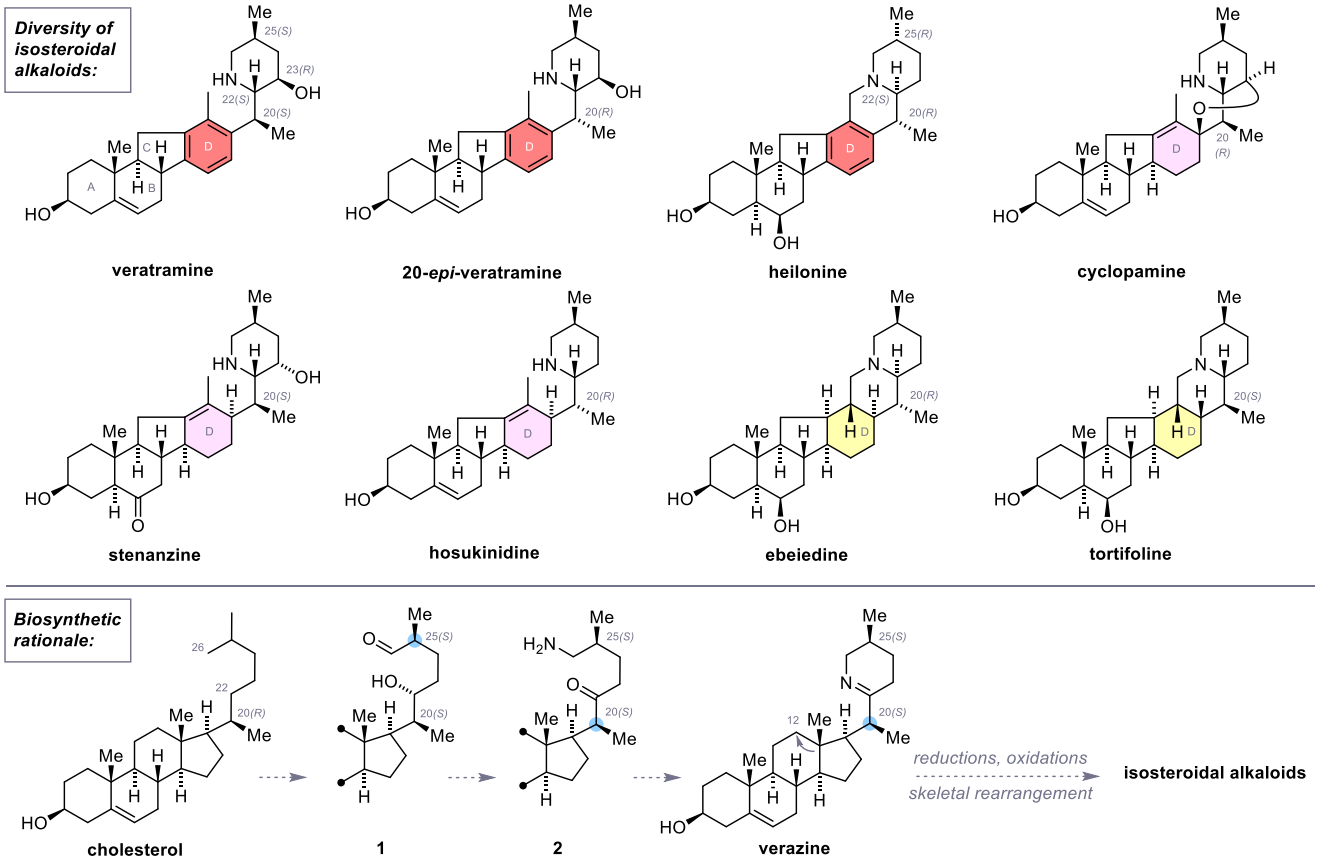

Scheme 1. A) Selected isosteroidal alkaloids with different degrees of saturation in the D ring and stereochemical variations. **B**) Initial steps of their biosynthesis. Easily epimerized stereocenters are indicated with a blue circle.

The occurrence of diastereomeric family members can be explained considering their biosynthesis (**Scheme 1B**). The biosynthetic pathway is known to proceed through cholesterol, all carbons of which are retained in the isosteroidal alkaloids.[5,6,7,8] It involves oxidations at C26 and C22 and features several epimerizable intermediates, such as the aldehyde **1**, the aminoketone **2**, and the D^1-piperideine **verazine**. Indeed, **20-*epi*-verazine** has been isolated in up to a 1:1 ratio relative to verazine in *Veratrum maackii*.[9] Reduction of the imine, oxidative activation at C12, Wagner-Meerwein type skeletal rearrangement, and further oxidations then lead to the isosteroidal alkaloids. An isomer of veratramine, proposed to be **20-*epi*-veratramine**, was reported in 1997.[10]

Given the prominent bioactivities and attractive structures of the isosteroidal alkaloids, it is no surprise that they have attracted considerable attention from the synthetic community, and especially so in recent years.[11-18] We have joined this effort, aiming at a convergent and diversifiable strategy that would provide maximal flexibility with respect to the saturation of the D ring and the stereocenters at C20 and on the piperidine ring (**Scheme 2**). Previous syntheses installed the D ring using aromatic starting materials (veratramine, Johnson;[11] veratramine, Gao;[12] heilonine, Dai[13]), biomimetic Meerwein-Wagner rearrangements (cyclopamine, Giannis;[14] veratramine and cyclopamine, Liu and Qin[15]), furan Diels-Alder reaction (zygadenine, Luo[16]), rhodium-catalyzed cyclotrimerization (heilonine, Rawal[17]), or ruthenium-catalyzed ring-closing metathesis (cyclopamine, Baran[18]). We decided to center our approach on an intramolecular Diels Alder reaction (IMDA), identifying 1,4-cyclohexadiene **3** as a key intermediate. In the forward direction, **3** could either be aromatized or selectively reduced at the less hindered double bond. Retrosynthetically, 1,4-cyclohexadiene **3** could be traced to dienyne **4**, via diastereoselective cycloaddition. This intermediate could stem from allylic phosphonate **5** and alkynal **6** via stereoselective olefination. Piperidine building block **5** and A/B ring decalin building block **6** are of approximately equal size and complexity, rendering our strategy highly convergent.

We now report a concise and convergent synthesis of veratramine and 20-*epi*-veratramine along these lines. The assembly of the piperidine building block began with enantiomerically pure *o*-bromo sulfonamide **8**, prepared from commercially available (*S*)-3-methyl piperidine (**7**, $9/g; **Scheme 3A**). Regioselective desaturation via C–H-activation gave the known phenylsulfonyl enamine **9** on a multigram scale.[19] Careful optimization of this step improved both its regioselectivity and yield from 3:1 to 5:1 and from 54% to 72%, respectively.

For the installation of the side chain, we initially followed a protocol developed by Taber.[20] Conversion of **9** into unstable bromohydrin **10,** followed by treatment with potassium hydride, and subsequent addition of crotyl magnesium chloride (**11)** gave piperidines **12α** and **12β** as an easily separated 1:1 mixture of diastereomers. As such, this procedure lacked stereoselectivity but it gave access to both desired epimers.

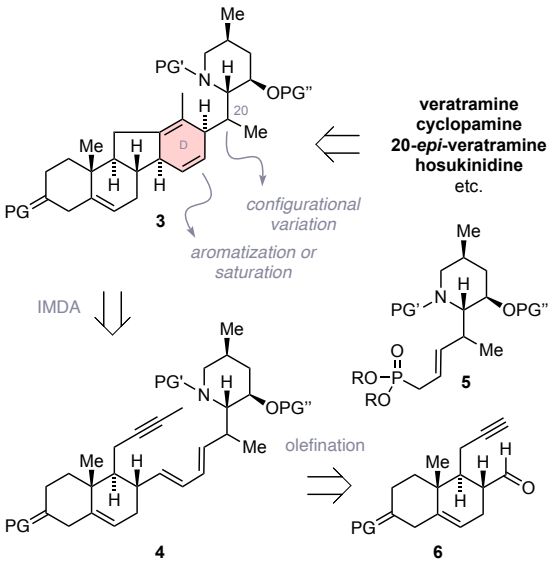

Scheme 2: Retrosynthetic analysis and identification of key building blocks for an IMDA approach. PG = protecting group.

For the 20*(R),* or α, series, we were able to develop a highly diastereoselective protocol. We hypothesized that the absence of stereoselectivity in the previous conditions resulted from the crotyl Grignard nucleophile existing as an equilibrating *E*:*Z* mixture due to rapid metallotropic shifts.[21] This led us to investigate configurationally stable nucleophiles, such as crotyl silanes. We also prepared *N*, *O* acetal **13** as an *N*-sulfonyl iminium electrophile precursor. Such electrophiles are known to react with simple allyl nucleophiles under Lewis acid catalysis;[22,23,24] however, minimal data were available to predict which crotyl isomer would afford the desired product. We reasoned that attack of *E*-but-2-en-1-yltrimethylsilane **14** onto the *N*-sulfonyl iminium ion through transition state **15** would provide the desired α-adduct (**Scheme 4**). Using **14** and $TiCl_4$ indeed gave the desired diastereomer as the major product, along with a facial isomer **16**, whose side-chain configuration could not be fully determined. The diastereomer **12β** was not observed under these conditions. We hypothesized that the facial selectivity with respect to the piperidine ring could be improved by increasing the steric bulk of the Lewis acid. Whereas alkoxy or cyclopentadienyl titanium species shut down reactivity, titanium tetrabromide increased the d.r. to 10:1. This reaction could be reliably performed on gram scale.

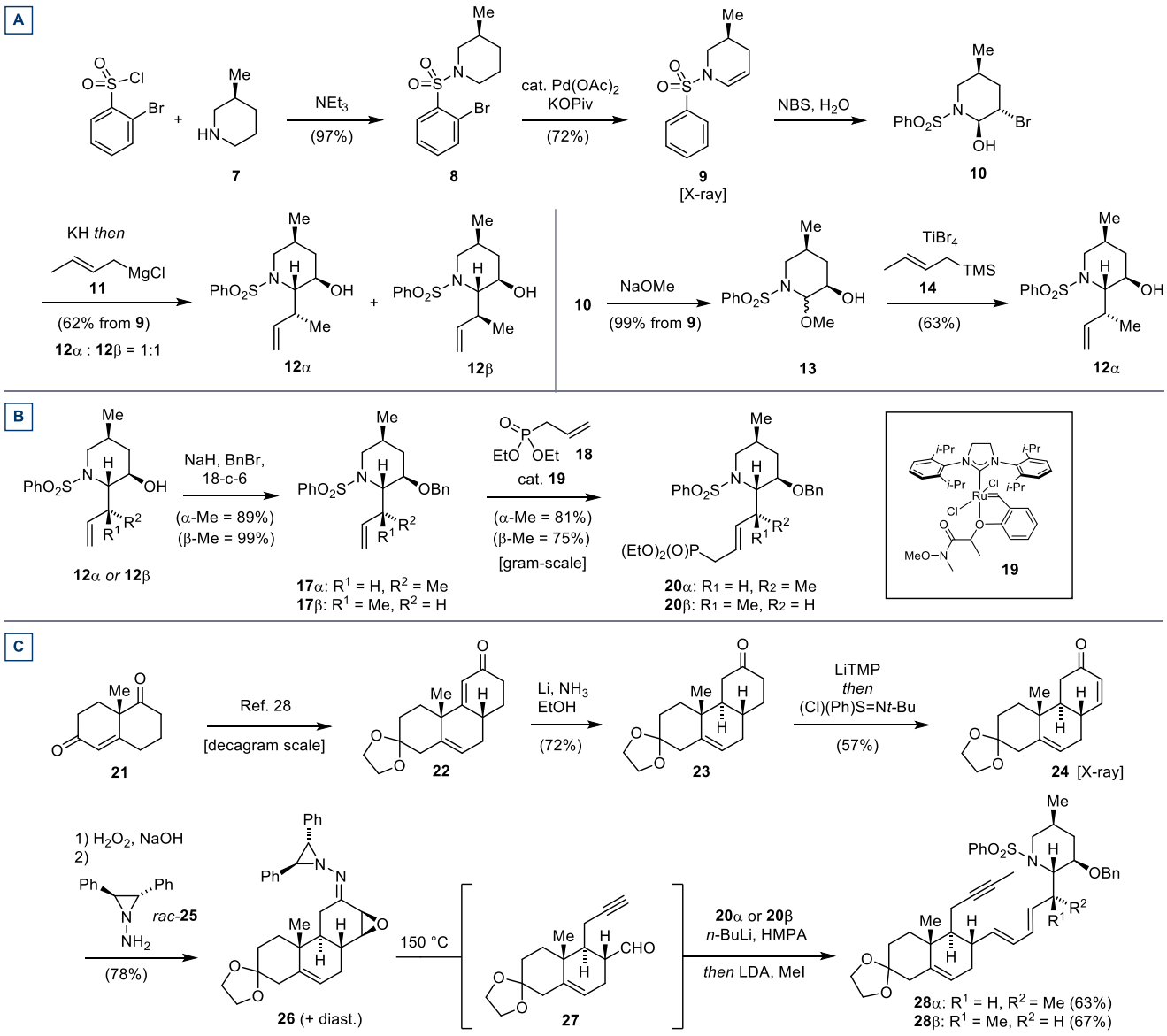

Scheme 3: Assembly and linkage of the key building blocks. **A**) Assembly of a chiral piperidine building block. **B**) Cross metathesis approach to allylic phosphonates. **C**) Synthesis of steroidal building block and coupling of the piperidyl and steroidal building blocks.

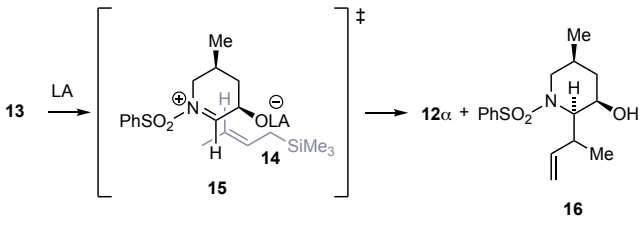

Lewis Acid	12α : 16
$TiCl_4$	1.9 : 1
BF_3	0.7 : 1
$Sc(OTf)_3$	n.d.
$CpTiCl_3$	n.d.
$Ti(Oi\text{-}Pr)_4$	n.d.
$TiBr_4$	>10 : 1

Scheme 4. Reaction design and optimization for the diastereoselective crotylation of *N*, *O* acetal **13**. For n.d., no product was detected.

To elaborate **12α,β** to the requisite allylic phosphonate building blocks of type **5**, we employed cross metathesis (**Scheme 3B**).[25,26] Following protection of alcohols **12α** and **12β** as benzyl ethers **17α** and **17β**, respectively, subjection to various Grubbs-type catalysts in the presence of diethyl allylphosphonate (**18**) at temperatures up to 70 °C gave minimal conversion. We hypothesized that catalyst decomposition occurred at higher temperatures, so we screened thermally stable NHC-ligated ruthenium complexes and found **19** ("Green Catalyst") to be best suited.[27] After optimization of catalyst addition, solvent,

https://doi.org/10.26434/chemrxiv-2024-ccrr6 **ORCID:** https://orcid.org/0000-0002-6782-6056

and stoichiometry, **20α** and **20β** could be reliably prepared on a gram scale.

The A/B ring building block of type **6** was accessed from the known tetracyclic enone **22**.[28] This compound is readily available on a decagram scale from Wieland Miescher ketone **(21**) via acetal protection and Robinson annulation (**Scheme 3C**). Net enone transposition with installation of the final methine stereocenter was accomplished in two steps. First, conjugate reduction gave ketone **23**, which features the thermodynamically more favorable *trans* decalin linkage. Then, regioselective desaturation was achieved via formation of the less-hindered enolate using the bulky lithium 2,2,6,6-tetramethylpiperidide followed by reaction with the oxidant *N*-*tert*-butylbenzenesulfinimidoyl chloride.[29,30] At this point, the configuration of enone **24** was confirmed via single crystal X-ray diffraction (XRD; **see SI**). To install both the aldehyde and the alkyne moieties simultaneously, we envisioned performing an Eschenmoser fragmentation. To this end, **24** underwent nucleophilic epoxidation to give an epoxy ketone as a single diastereomer that was used without purification. Initial attempts at the Eschenmoser fragmentation using standard conditions (e.g., $TsNHNH_2$/AcOH) resulted in tosylhydrazine condensation with the desired ynal. To avoid this issue, we investigated the thermal variant of the Eschenmoser fragmentation.[31] The isolable imino aziridine **26** was formed as an inconsequential mixture of diastereomers using racemic hydrazine **25**, then subjected to thermolysis. After optimization of solvent and heating methods, we found that microwave heating at 150 °C cleanly afforded ynal **27** with the correct *anti* relationship of the propargyl and formyl substituents. Under these conditions, the only byproducts are nitrogen and stilbene, so the crude mixture could be used immediately following concentration. Nevertheless, **27**, could be isolated and fully characterized (see SI). Crude **27** could be linked with phosphonate **20** through Horner-Wadsworth-Emmons olefination.[32] The terminal alkyne of the resulting intermediate was methylated in the same reaction pot to yield **28**. This sequence was highly effective and gave both diastereomers **28α** and **28β** in good overall yield from hydrazone **26**.

The stage was now set for the IMDA reaction that would construct the D ring (**Scheme 5A**). Attempts at thermal cyclization of **28α** proved ineffective – minimal conversion was observed at 130 °C and decomposition rapidly occurred at 150 °C. We therefore focused on rhodium and nickel catalyzed dienyne IMDA reactions.[33,34,35] Using $[Rh(COD)Cl]_2$ in trifluoroethanol (TFE),[36] we observed formation of a single 1,4-cyclohexadiene as determined by a characteristic AB system in the ^1H NMR spectrum. Its structure was tentatively assigned as **29** based on a conformational analysis of the precursor and mechanistic considerations. We also investigated Ni^0-catalyzed cyclizations using the recently introduced stable Ni^0 source $Ni(^{4\text{-}tBu}stb)_3$.[37] This catalyst produced **29** alongside a diastereomer. Thus, we sought to unambiguously characterize **29** via X-ray diffraction to determine the orientation of the two newly installed methine stereocenters. Whereas numerous attempts to crystallize **29** failed, removal of the *N*-sulfonyl and *O*-benzyl groups gave crystalline **33** (**Scheme 5A**, inset). Single crystal XRD corroborated the anticipated stereochemistry (**Scheme 5C**, left).

We discovered two additional important nuances while optimizing the rhodium-catalyzed IMDA reaction: cationic rhodium sources tended to (1) produce some aromatized product and (2) effect deketalization and double bond migration in the presence of trace water. Since we needed to aromatize the D-ring and hydrolyze the dioxolane protecting group anyways, we decided to optimize for this reactivity by adding $AgSbF_6$ to abstract chloride and form a cationic rhodium complex *in situ*. After screening several ligands and potential hydrogen acceptors, we also found that addition of diethyl fumarate (**30**) significantly improved the yield of the aromative IMDA reaction. Notably, exposure of the intermediary 1,4-cyclohexadiene **29** to more conventional dehydrogenation reagents, such as DDQ, gave poor results. Finally, we found that deliberate addition of 25 equivalents of water hydrolyzed the ketal and isomerized the double bond, providing aromatic enone **31** from dienyne **28α** in a single operation.

The synthesis of 20-*epi*-veratramine was completed through stereoselective conversion of enone **31** to homoallylic alcohol **32** *via* a dienyl acetate (**Scheme 5B**). Reductive debenzylation and sulfonylation under dissolving metal conditions then gave our first synthetic target. Its epimer was synthesized analogously. Rhodium-catalyzed aromative IDMA reaction with concomitant deprotection and double bond migration gave enone **34** in one operation from 1,4-cyclohexadiene **28β**. Installation of the homoallylic alcohol in the A/B ring yielded **35** and reductive deprotection then delivered veratramine.

In the case of veratramine, our analytical data were identical in all respects with published data.[38] However, our sample of 20-*epi*-veratramine did not match the reported NMR or optical rotation data (see SI).[38] Thus, we crystallized both veratramine and 20-*epi*-veratramine for analysis via single crystal XRD. The crystallographic analysis confirmed our assignment of each natural product (**Scheme 5C**). Whereas the structures of the steroidal cores remain essentially unperturbed, the configuration at C20 dramatically influences the orientation of the piperidyl ring. To avoid $A^{1,3}$ strain, the C–H bond at C20 is essentially coplanar with the aromatic ring. This orients the piperidyl moiety downwards in 20-*epi*-veratramine and upwards in veratramine. The true structure of the isosteroidal alkaloid proposed to be 20-*epi*-veratramine remains to be determined. However, the C23-*O*-glucoside of 20-*epi*-veratramine has been isolated, and its spectroscopic data are in good agreement with our sample, with minor, predictable deviations for resonances adjacent to the site of *O*-glycosylation.[39] Thus, we believe that 20-*epi*-veratramine could be a *bona fide* natural product.[40]

In sum, we have developed a short and efficient synthesis of 20-*epi*-veratramine and veratramine that compares well with previous approaches. It proceeds in 11 linear steps from commercially available (*S*)-3-methylpiperidine or in 9 linear steps from the known hydrophenanthrenone **22** (13 from **21**). Access to 1,4-cyclohexadiene **29** and its epimer

will allow us to extend our program towards additional isosteroidal alkaloids, such as stenanzine and hosukinidine. The IMDA approach could be further diversified to reach hexacylic isosteroidal alkaloids, such as heilonine, ebeiedine, and tortifoline. These studies will support pharmacological exploration into this diverse family of alkaloids, including the opportunity to study the bioactivities of the 20*(R)* series.

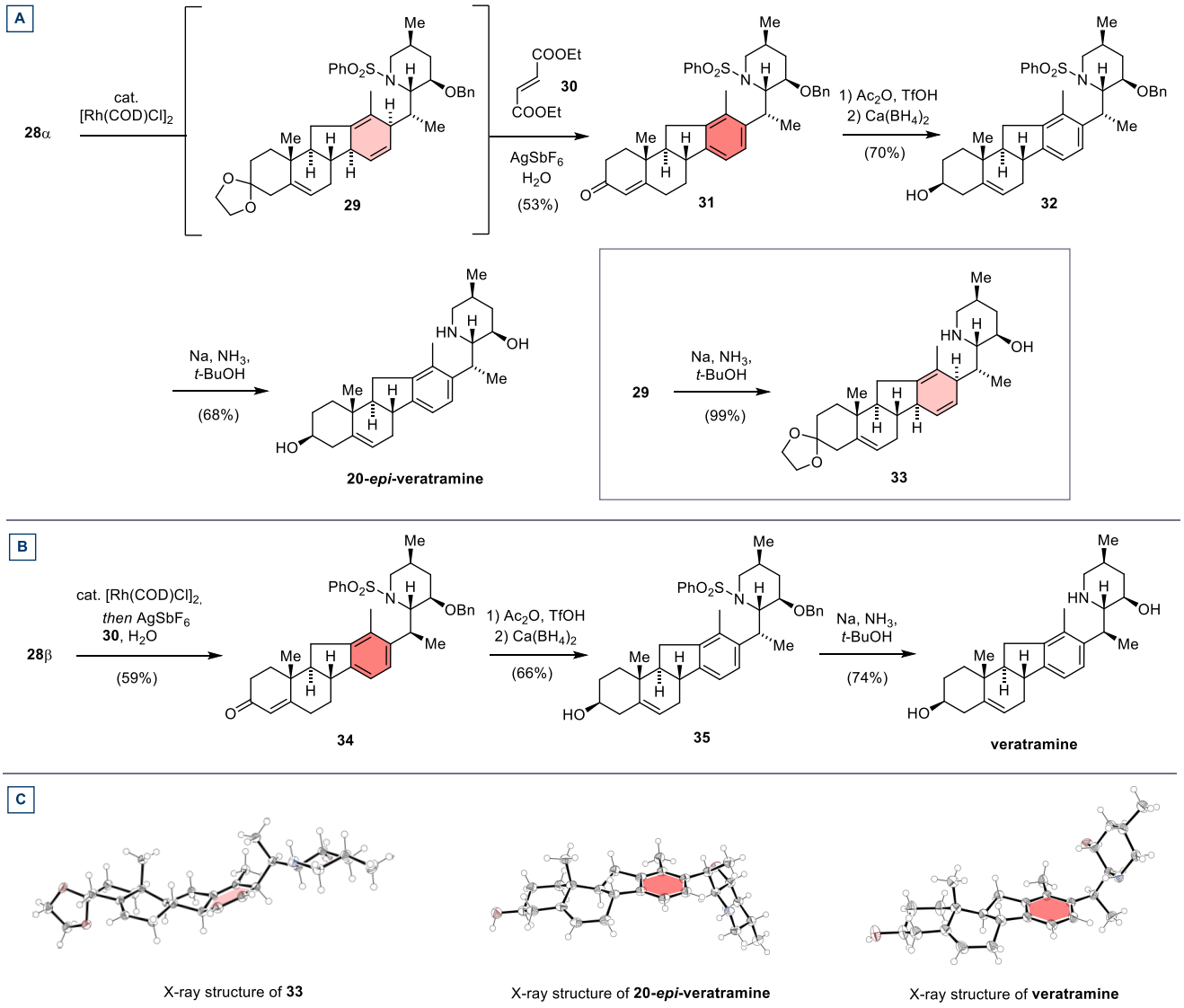

Scheme 5: Construction of the D ring and completion of the total syntheses of **A**) 20-*epi*-veratramine, and **B)** veratramine. **C**) Corroborating single crystal X-ray diffraction analysis.

ASSOCIATED CONTENT

Supporting Information

The Supporting Information contains experimental details and characterization data for all new compounds.

CCDC 2404193, 2404194, 2404195, 2404196, and 2404197 contain the supplementary crystallographic data for this paper. These data can be obtained for free at www.ccdc.cam.ac.uk/data_request/cif, or by contacting The Cambridge Crystallographic Data Centre, 12 Union Road, Cambridge CB2 1EZ, UK; fax: +44 1223 336033; email: data_request@ccdc.cam.ac.uk.

ACKNOWLEDGMENTS

We gratefully acknowledge financial support through the National Science Foundation (CHE-1900154 to DHT). Michael D. Zott is supported by the Arnold and Mabel Beckman Foundation as an Arnold. O. Beckman Postdoctoral Fellow. X-ray crystallography was performed by Dr. Michael R. Gau and Dr. Alexandra M. Bacon (UPenn). We thank Prof. Douglass F. Taber for valuable discussions.

Graphical Abstract:

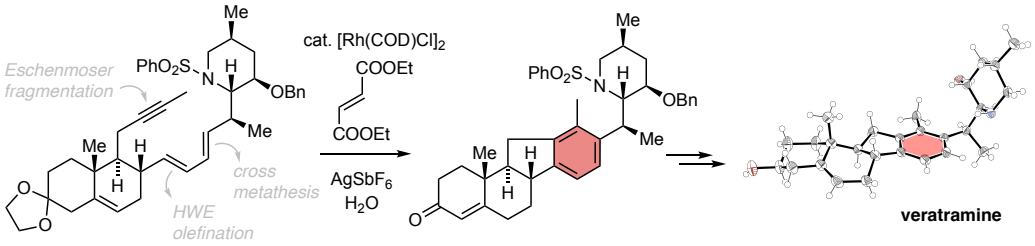

REFERENCES

[1] Xiang, M.-L.; Hu, B.-Y.; Qi, Z.-H.; Wang, X.-N.; Xie, T.-Z.; Wang, Z.-J.; Ma, D.-Y.; Zeng, Q; Luo, X.-D. Chemistry and Bioactivities of Natural Steroidal Alkaloids. *Nat. Prod. Bioprospect.* **2022**, *12*, 23.

[2] Heretsch, P.; Tzagkaroulaki, L.; Giannis, A. Cyclopamine and Hedgehog Signaling: Chemistry, Biology, Medical Perspectives. *Angew. Chem., Int. Ed.* **2010**, *49*, 3418–3427.

[3] Heretsch, P.; Giannis, A. *The Veratrum and Solanum Alkaloids*; The Alkaloids: Chemistry and Biology; Academic Press: 2015; Vol. 74, pp 201–232.

[4] Jiang, Q.-W.; Chen, M.-W.; Cheng, K.-J.; Yu, P.-Z.; Wei, X.; Shi, Z. Therapeutic Potential of Steroidal Alkaloids in Cancer and Other Diseases. *Med. Res. Rev.* **2016**, *36*, 119–143.

[5] Winegar, P. H.; Hudson, G. A.; Dell, L. B.; Astolfi, M. C. T.; Reed, J.; Payet, R.D.; Ombredane, H. C. J.; Iavarone, A. T.; Chen, Y.; Gin, J. W.; Petzold, C. J.; Osbourn, A. E.; Keasling, J. D. Verazine Biosynthesis from Simple Sugars in Engineered *Saccharomyces cerevisiae*. *Metab. Eng.* **2024**, *85*, 145–158.

[6] Augustin, M. M.; Ruzicka, D. R.; Shukla, A. K.; Augustin, J. M.; Starks, C. M.; O'Neil-Johnson, M.; McKain, M. R.; Evans, B. S.; Barrett, M. D.; Smithson, A.; Wong, G. K.; Deyholos, M. K.; Edger, P. P.; Pires, J. C.; Leebens-Mack, J. H.; Mann, D. A.; Kutchan, T. M. Elucidating Steroid Alkaloid Biosynthesis in *Veratrum californicum*: Production of Verazine in Sf9 cells. *Plant J.* **2015**, *82*, 991–1003.

[7] Chandler, C. M.; McDougal, O. M. Medicinal History of North American *Veratrum*. *Phytochem. Rev.* **2014**, *13*, 671–694.

[8] Kaneko, K.; Mitsuhashi, H.; Hirayama, K.; Yoshida, N. Biosynthesis of C-Nor-D-Homo-Steroidal Alkaloids from Acetate-1-^{14}C, Cholesterol-4-^{14}C and Cholesterol-26-^{14}C in *Veratrum grandiflorum*. *Phytochem*. **1970**, *9*, 2489–2495.

[9] Han, X.; Rüegger, H. Epimeric(20R,20S)-Verazine Isolated from *Veratrum maackii*: Two-Dimensional NMR Studies and Total Assignment of ^{1}H- and ^{13}C-Resonances. *Planta Med.* **1992**, *58*, 449–453.

[10] Tezuka, Y.; Kikuchi, T.; Zhao, W.; Chen, J.; Guo, Y. Two New Steroidal Alkaloids, 20-Isoveratramine and Verapatuline, from the Roots and Rhizomes of *Veratrum patulum*. *J. Nat. Prod.* **1998**, *61*, 1078–1081.

[11] Johnson, W. S.; DeJongh, H. A. P.; Coverdale, C. E.; Scott, J. W.; Burckhardt, U. Synthesis of Veratramine. *J. Am. Chem. Soc.* **1967**, *89*, 4523–4524.

[12] Shao, H.; Liu, W.; Liu, M.; He, H.; Zhou, Q.-L.; Zhu, S.-F.; Gao, S. Asymmetric Synthesis of Cyclopamine, a Hedgehog (Hh) Signaling Pathway Inhibitor. *J. Am. Chem. Soc.* **2023**, *145*, 25086–25092.

[13] Jin, Y.; Hok, S.; Bacsa, J.; Dai, M. Convergent and Efficient Total Synthesis of (+)-Heilonine Enabled by C–H Functionalizations. *J. Am. Chem. Soc.* **2024**, *146*, 1825–1831.

[14] Giannis, A.; Heretsch, P.; Sarli, V.; Stößel, A. Synthesis of Cyclopamine Using a Biomimetic and Diastereoselective Approach. *Angew. Chem., Int. Ed.* **2009**, *48*, 7911–7914.

[15] Hou, W.; Lin, H.; Wu, Y.; Li, C.; Chen, J.; Liu, X.-Y.; Qin, Y. Divergent and Gram-Scale Syntheses of (–)-Veratramine and (–)-Cyclopamine. *Nat. Commun.* **2024**, *15*, 5332.

[16] Guo, Y.; Lu, J.-T.; Fang, R.; Jiao, Y.; Liu, J. and Luo, T. Enantioselective Total Synthesis of (–)-Zygadenine. *J. Am. Chem. Soc.* **2023**, *145*, 20202–20207.

[17] Cassaidy, K. J.; Rawal, V. H. Enantioselective Total Synthesis of (+)-Heilonine. *J. Am. Chem. Soc.* **2021**, *143*, 16394–16400.

[18] Sofiadis, M.; Xu, D.; Rodriguez, A. J.; Nissl, B.; Clementson, S.; Petersen, N. N.; Baran, P. S. Convergent Total Synthesis of (–)-Cyclopamine. *J. Am. Chem. Soc.* **2023**, *145*, 21760–21765.

[19] Bheeter, C. B.; Jin, R.; Bera, J. K.; Dixneuf, P. H.; Doucet, H. Palladium-Catalysed Dehydrogenative *sp*^{3} C–H Bonds Functionalisation into Alkenes: A Direct Access to *N*-Alkenylbenzenesulfonamides. *Adv. Synth. Catal.* **2014**, *356*, 119–124.

[20] Taber, D. F.; Dematteo, P. W. A Piperidine Chiron for the *Veratrum* Alkaloids. *J. Org. Chem.* **2012**, *77*, 4235–4241.

[21] Hoffmann, R. W. Diastereogenic Addition of Crotylmetal Compounds to Aldehydes. *Angew. Chem. Int. Ed.* **1982**, *21*, 555–566.

[22] Åhman, J.; Somfai, P. Carbon–Carbon Bond Formation via N-Tosyliminium Ions. *Tetrahedron* **1992**, *48*, 9537–9544.

[23] Okitsu, O.; Suzuki, R.; Kobayashi, S. Efficient Synthesis of Piperidine Derivatives. Development of Metal Triflate-Catalyzed Diastereoselective Nucleophilic Substitution Reactions of 2-Methoxy- and 2-Acyloxypiperidines. *J. Org. Chem.* **2001**, *66*, 809–823.

[24] Gutierrez, D. A.; Fettinger, J.; Houk, K. N.; Ando, K.; Shaw, J. T. Diastereoselective Addition of Prochiral Nucleophilic Alkenes to α-Chiral *N*-Sulfonyl Imines. *Org. Lett.* **2022**, *24*, 1164–1168.

[25] Chatterjee, A. K.; Choi. T.-L.; Grubbs, R. H. Synthesis of Vinyl- and Allylphosphonates by Olefin Cross-Metathesis. *Synlett* **2001**, 1034–1037.

[26] Rahn, N.; Kalesse, M. The Total Synthesis of Chlorotonil A. *Angew. Chem. Int. Ed.* **2008**, *47* 597–599.

[27] Skowerski, K.; Kasprzycki, P.; Bieniek, M.; Olszewski, T. K. Efficient, Durable and Reusable Olefin Metathesis Catalysts with High Affinity to Silica Gel. *Tetrahedron* **2013**, *69*, 7408–7415.

[28] Smith III, A. B.; Leenay, T. L. Indole Diterpene Synthetic Studies. 5. Development of a Unified Synthetic Strategy; A Stereocontrolled, Second-Generation Synthesis of (-)-Paspaline. *J. Am. Chem. Soc.* **1989**, *111*, 5761–5768.

[29] Kapras, V.; Vyklicky, V.; Budesinsky, M.; Cisarova, I.; Vyklicky, L.; Chodounska, H.; Jahn, U. Total Synthesis of ent-Pregnanolone Sulfate and Its Biological Investigation at the NMDA Receptor. *Org. Lett.* **2018**, *20*, 946–949.

[30] Mukaiyama, T.; Matsuo, J.; Yanagisawa, M. A New and Efficient Method for Oxidation of Various Alcohols by Using *N*-*tert*-Butyl Phenylsulfinimidoyl Chloride. *Bull. Chem. Soc. Jpn.* **2000**, *29*, 1072–1073.

[31] Felix, D.; Muller, R. K.; Horn, U.; Joos, R.; Schreiber, J.; Eschenmoser, A. α,β-Epoxyketone to Alkynone Fragmentation II. Pyrolytic Decomposition of Hydrazones from α,β-Epoxyketones and N-Aminoaziridines. *Helv. Chim. Acta* **1972**, *55*, 1276–1319.

[32] Wang, Y.; West, F. G. A Convenient Method for the Synthesis of Terminal (E)-1,3-Dienes. *Synthesis* **2002**, 99–103.

[33] Wender, P.A.; Croatt, M.P.; Deschamps, N.M. C–C Bond Formation (Part 1) by Addition Reactions: Higher-Order Cycloadditions in Comprehensive Organometallic Chemistry III. **2007**, 603–647.

[34] Wender, P. A.; Smith, T. E. Transition Metal-Catalyzed Intramolecular [4 + 2] Cycloadditions: Mechanistic and Synthetic Investigations. *Tetrahedron* **1998**, *54*, 1255–1275.

[35] Jolly, R. S.; Luedtke, G.; Sheehan, D.; Livinghouse, T. Novel Cyclization Reactions on Transition Metal Templates. The Catalysis of Intramolecular [4+2] Cycloadditions by Low-Valent Rhodium cComplexes. *J. Am. Chem. Soc.* **1990**, *112*, 4965–4966.

[36] Zhang, W.; Zhou, Z.-X.; Zhu, X.-J.; Sun, Z.-H.; Dai, W.-M.; Li, C.-C. Asymmetric Total Synthesis of the Highly Strained 4β-Acetoxyprobotryane-9β,15α-diol. *J. Am. Chem. Soc.* **2020**, *142*, 19868–19873.

[37] Nattmann, L.; Cornella, J. Ni($^{4\text{-tBu}}$stb)$_3$: A Robust 16-Electron Ni(0) Olefin Complex for Catalysis. *Organometallics* **2020**, *39*, 3295–3300.

[38] Tezuka, Y.; Kikuchi, T.; Zhao, W.; Chen, J.; Guo, Y. Two New Steroidal Alkaloids, 20-Isoveratramine and Verapatuline, from the Roots and Rhizomes of *Veratrum patulum*. *J. Nat. Prod.* **1998**, *61*, 1078–1081.

[39] Irsch, E.-M.; Pachaly, P.; Breitmaier, E.; Sin, K.-S. Alkaloide aus *Veratrum patulum*, I. Isolierung und Strukturaufklärung neuer Steroidalkaloidglycoside. *Liebigs Ann. Chem.* **1993**, *1993*, 281–285.

[40] Hetzler, B. E.; Trauner, D.; Lawrence, A. L. Natural Product Anticipation through Synthesis. *Nat. Rev. Chem.* **2022**, *6*, 170–181.